Journal of Extracellular Vesicles

co-action PUBLISHING

ORIGINAL RESEARCH ARTICLE

Diversity of extracellular vesicles in human ejaculates revealed by cryo-electron microscopy

Johanna L. Höög* and Jan Lötvall

Krefting Research Centre, Institute of Medicine, Sahlgrenska Academy, University of Gothenburg, Gothenburg, Sweden

Human ejaculates contain extracellular vesicles (EVs), that to a large extent are considered to originate from the prostate gland, and are often denominated "prostasomes." These EVs are important for human fertility, for example by promoting sperm motility and by inducing immune tolerance of the female immune system to the spermatozoa. So far, the EVs present in human ejaculate have not been studied in their native state, inside the seminal fluid without prior purification and isolation procedures. Using cryo-electron microscopy and tomography, we performed a comprehensive inventory of human ejaculate EVs. The sample was neither centrifuged, fixed, filtered or sectioned, nor were heavy metals added. Approximately 1,500 extracellular structures were imaged and categorized. The extracellular environment of human ejaculate was found to be diverse, with 5 major subcategories of EVs and 6 subcategories of extracellular membrane compartments, including lamellar bodies. Furthermore, 3 morphological features, including electron density, double membrane bilayers and coated surface, are described in all subcategories. This study reveals that the extracellular environment in human ejaculate is multifaceted. Several novel morphological EV subcategories are identified and clues to their cellular origin may be found in their morphology. This inventory is therefore important for developing future experimental approaches, and to interpret previously published data to understand the role of EVs for human male fertility.

Keywords: *exosomes*; *microvesicle*; *microparticle*; *seminal fluid*; *male fertility*; *surface coat*; *spikes*; *double bilayer*; *cryo-electron tomography*

Responsible Editor: Eva-Maria Krämer-Albers, Johannes Gutenberg University, Germany.

*Correspondence to: Johanna L. Höög, Krefting Research Centre, Institute of Medicine, Sahlgrenska Academy, University of Gothenburg, PO Box 424, SE-405 30 Gothenburg, Sweden, Email: Johanna.hoog@gu.se

To access the supplementary material to this article, please see Supplementary files under 'Article Tools'.

Received: 29 May 2015; Revised: 4 September 2015; Accepted: 11 October 2015; Published: 11 November 2015

The human ejaculate is a complex liquid, consisting of a mixture of spermatozoa, carbohydrates, proteins and extracellular vesicles (EVs). EVs are small vesicles released by all cells examined to date (1) and are common components of many body fluids, including saliva, blood, urine and human breast milk (2,3). They are known to carry many different protein cargoes, as well as a mixture of RNA species (4–6). EVs are important in cell-to-cell communication in a wide range of biological processes, especially in disease models such as the formation and progression of cancer (7–8). Relatively little is known about EVs in healthy processes and homeostasis.

The EVs in seminal fluid were first described in the 1970s (9,10) and were named prostasomes, because of their origin in the acinar cells in the prostate (11,12). However, as the epididymis epithelium and other cellular compartments in the male genital tract produce EVs that are released into the seminal fluid (13–15), we will here use the term "EVs" as a collective name for all vesicles found in human ejaculate.

EVs are known to fuse with spermatozoa (16,17) and their role in seminal fluid is diverse and extensively studied [reviewed in (15,18–20)]. Briefly, the EVs enhance sperm motility (21,22), aide semen liquefaction, prevent microbial infections (23,24), facilitate blood coagulation (25) and mediate immunosuppression in the female's genital tract to avoid anti-spermatozoa immunity (26,27). Seminal EVs have also been shown to have great potential as biomarkers for detection and diagnosis of prostate cancer (28).

The EVs in ejaculate are 150–200 nm in diameter (11,29) with a bilayer high in cholesterol and sphingomyelin (30),

Citation: Journal of Extracellular Vesicles 2015, **4**: 28680 - http://dx.doi.org/10.3402/jev.v4.28680

a membrane composition that greatly differs to that of spermatozoa plasma membranes (17).

Cryo-electron microscopy is a technique that allows visualization of nanosized structures without prior fixation or addition of heavy metals for contrast. The sample is therefore visualized as close to its native state as possible (31,32). Isolated EVs from human ejaculates have already been studied using cryo-electron microscopy, but only after several isolation and purification steps, to remove spermatozoa (33). In that study, the investigators describe 3 morphologically distinct subpopulations of vesicles.

To define the morphology of all types of EVs in human ejaculates, we performed cryo-electron microscopy on totally unaltered material. By this approach, we can make an inventory of the *whole* population of EVs in the unaltered human semen. We reveal a greater diversity of EV morphologies than previously described in any single human body fluid and are able to visualize vesicular fusion or budding at the level of the human sperm tail.

Materials and methods

Sample preparation

Seven different ejaculates from one healthy donor (defined as having produced offspring) were collected according to the WHO's guidelines for sperm collection (34) and frozen unperturbed. A Vitrobot climate controlled plunge freezer (FEI Company Ltd, Eindhoven, The Netherlands) was used within 1–3 hours post-ejaculation. After freezing, remaining cells were examined under the light microscope, where their motility ensured that viable cells had been frozen.

Cryo-electron microscopy and tomography

Cryo-electron microscopy was performed as in (35,36). In brief, images (electron dose of $\sim 25\ e^{-}/Å^2$; -4 to -6 µm defocus) were acquired at 27,500 × on a Tecnai F30 electron microscope (FEI Company Ltd.) operated at 300 kV. The detector was a GATAN UltraCam, lens-coupled, 4 K CCD camera (binned by 2) attached to a Tridiem Gatan Image Filter (GIF: operated at zero-loss mode with an energy window of 20 eV; Gatan, Inc., Pleasanton, CA, USA). For cryo-electron tomography, tilt series were acquired at -4 or -6 µm defocus, every 1.5 degree (± 60 degrees) using serialEM software (37). The total electron dose was kept at 80–120 $e^{-}/Å^2$.

Image analysis and quantification

All vesicles contained within the images (in grid holes as well as on the carbon support film) were measured using the IMOD program. Vesicles contained within other vesicles, membrane compartments or vesicle sacs were not measured separately. Vesicles located inside broken structures, such as inside incomplete vesicles, were considered their own entity and measured individually. Oval vesicles and tubules were measured along their long axis. The images were centred around, or in the vicinity of ~30 spermatozoa.

Results

Different subcategories of extracellular particles and vesicles found in human ejaculate

We have examined 755 cryo-electron microscopy images to build a structural inventory of different extracellular non-spermatozoa structures in human ejaculates. The seminal microenvironment was generally complex not only with several different categories of EVs but also with the presence of tubules, particles and intricate membrane structures (Fig. 1a, b). All the structures completely contained within the images were measured and divided into subcategories. An initial analysis of 808 particles showed that 90% of the structures present were small electron dense particles, often with a thin, peripheral and even more electron dense lining of 2–2.5 nm thickness surrounding it (Fig. 1c, d and Supplementary Fig. S1). Due to the lack of a membrane bilayer, we call these structures "particles." Because of the abundance of small electron dense particles, we subsequently measured only the membranous structures found in ejaculate in all remaining images (Fig. 1e).

In total, we found 11 subcategories of membrane structures, of which 59% were single vesicles but 41% consisted of more multifaceted assemblies (Fig. 1f). Vesicles are shown in Fig. 2, and all other membrane compartments are shown in Figs. 3–5.

Category 1: single vesicles

Single vesicles have a bilayer that is 5 nm thick, and these are the most prevalent EVs (Fig. 2a).

Category 2: oval vesicles

These vesicles are reminiscent of the single vesicles but are simply oval in shape (Fig. 2b).

Category 3: double vesicles

These vesicles contain a smaller vesicle inside of a larger vesicle, both carrying a lipid bilayer (Figs. 1h, i and 2c).

Category 4: double special vesicles

The double special vesicles have a larger diameter than the double vesicles (*t*-test, $P < 0.001$). The larger vesicle contains electron dense material and carries inside its cytoplasm another smaller electron translucent vesicle that is often deformed into a bean or half-moon shape (Fig. 2d).

Category 5: triple to 6 vesicles

This subgroup of vesicles varies morphologically. Some of these EVs consist of 2 small vesicles stuck into a larger

Citation: Journal of Extracellular Vesicles 2015, **4**: 28680 - http://dx.doi.org/10.3402/jev.v4.28680

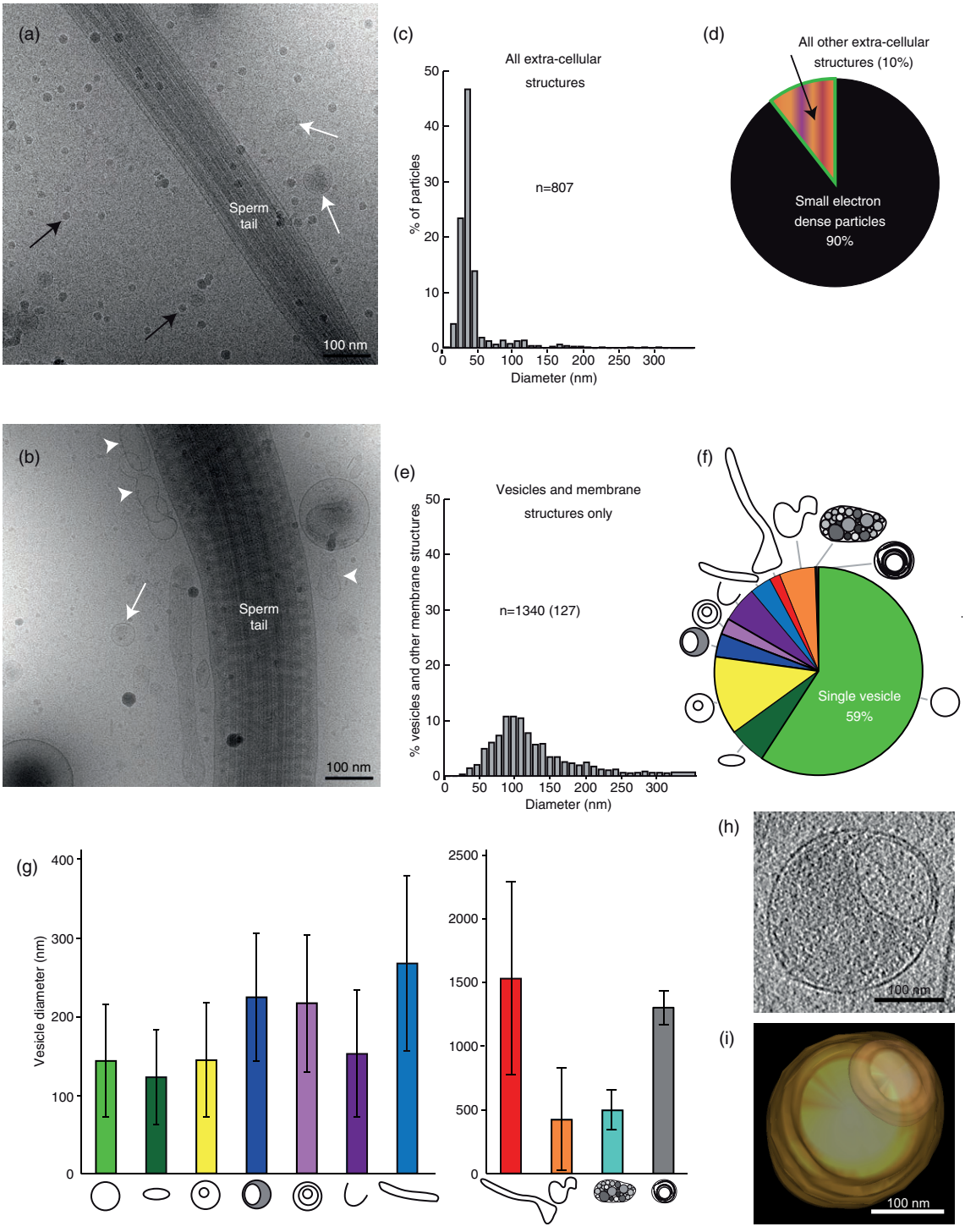

Fig. 1. Vastly diverse vesicles and other membrane compartments found in human ejaculate. (a) A cryo-electron micrograph of human sperm tail surrounded by small, electron dense particles (black arrows) as well as EVs (white arrows). (b) A cryo-electron micrograph of a sperm tail, EVs (white arrows) and other membrane compartments (white arrowheads). (c) The size distribution of all particles and membranous compartments in human ejaculates. (d) Prevalence of particles and all membranous compartments in the seminal fluid. (e) The size distribution of EVs and membranous compartments in human ejaculate from all 7 ejaculates pooled (excluding particles lacking lipid bilayer; number in brackets represents the amount of vesicles with a larger diameter than displayed in this graph). (f) The prevalence of each EV or membrane compartment. Clockwise: single vesicles, oval vesicle, double vesicle, double special vesicle, triple to 6 vesicles, incomplete vesicles, small tubules, large tubules, pleomorphic membrane structures, vesicle sacs and lamellar bodies. (g) Sizes of vesicles/membrane compartments in each subcategory (average and standard deviation). (h) A 10-nm-thick slice from a tomographic reconstruction of a double special vesicle. (i) 3D model of the vesicle shown in h.

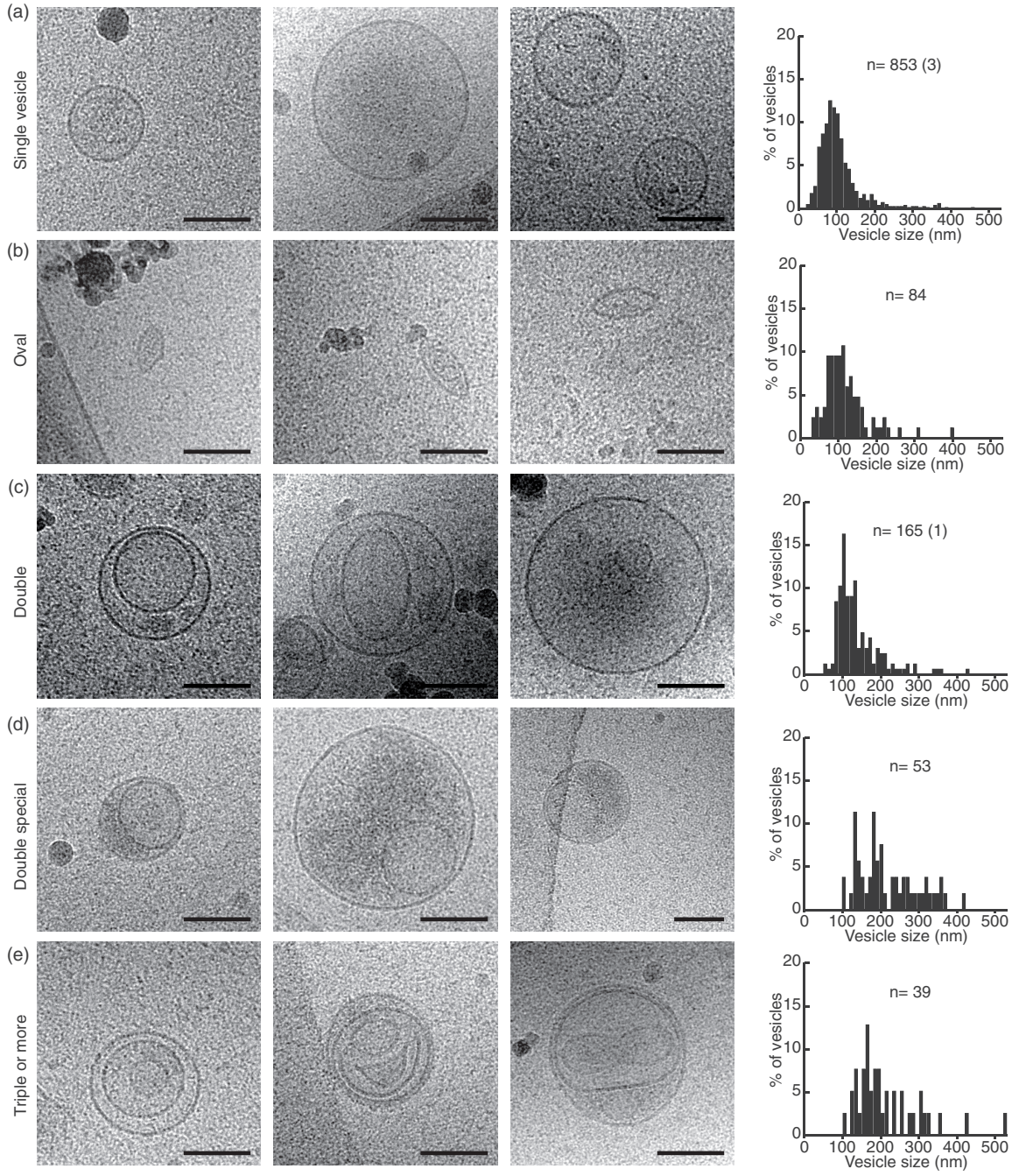

Fig. 2. Gallery of extracellular vesicle subcategories. (a–e) Three cryo-electron micrographs are shown for each category, followed by the EV size distribution of that subcategory. n = sample size (amount of vesicles above 500 nm in diameter). Scale bars = 50 nm.

one, and some are more complex arrangements of one larger vesicle containing single and/or double vesicles (Fig. 2e).

Category 6: incomplete vesicles

These half-circle shaped membrane structures often have electron dense material located within them, as well as outside of them (Fig. 3a). This category probably represents broken/incomplete vesicles, originating from several of the other subcategories.

Category 7: small tubules

These thin, often edgy looking tubules are commonly present in close proximity to sperm tails (Fig. 3b). They sometimes carry double membrane bilayers (first and third image in Fig. 3b).

Category 8: large tubules

These tubule-shaped membrane compartments are thicker and much longer (0.650–2.3 μm). Only tubules completely

Citation: Journal of Extracellular Vesicles 2015, **4**: 28680 - http://dx.doi.org/10.3402/jev.v4.28680

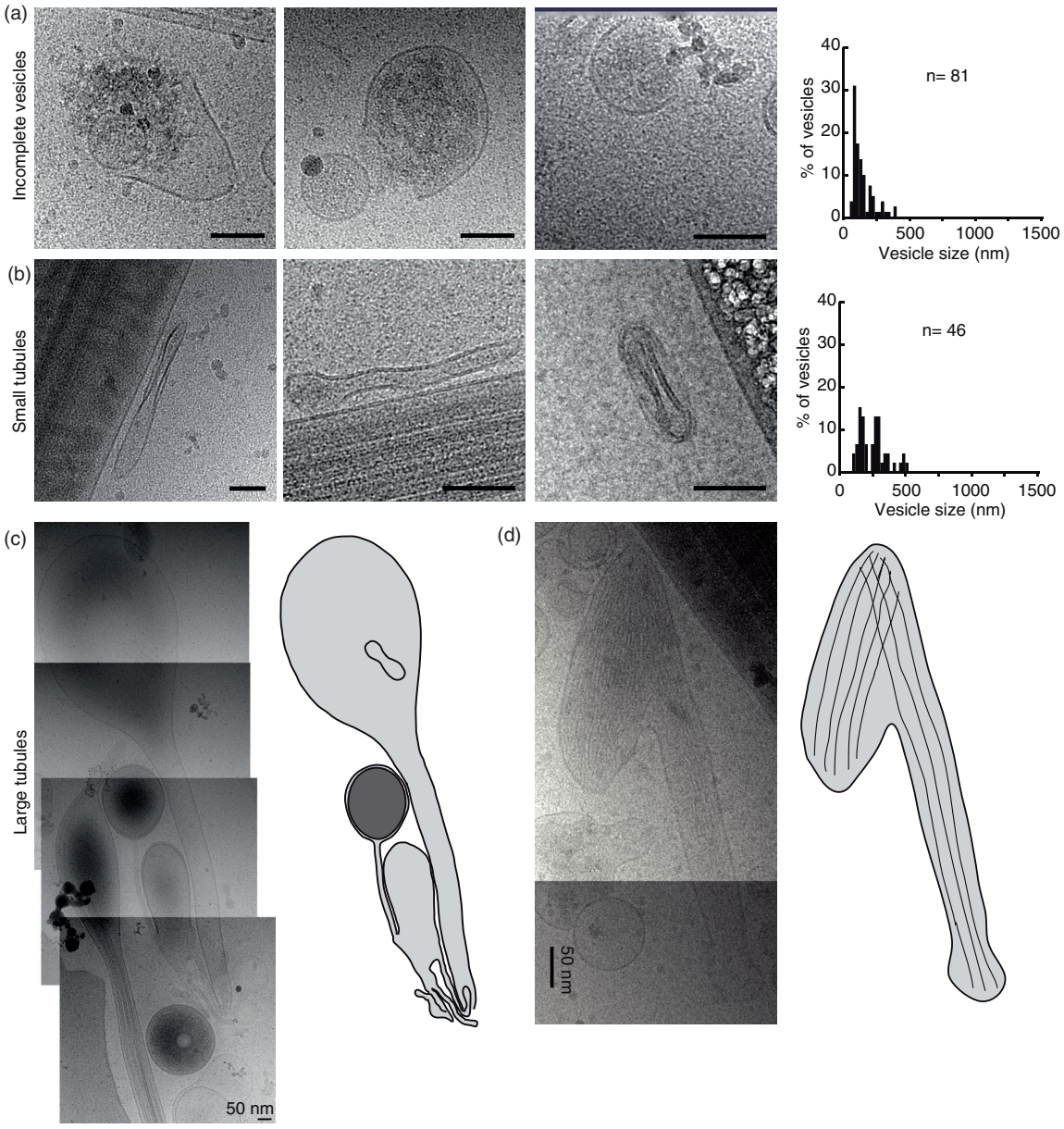

Fig. 3. Gallery of different membrane compartments. (a) Incomplete vesicles and their size distribution. (b) Thin tubules and their size distributions. (c) Large tubule, captured over several overlapping images and line drawings to show their complicated internal relations. (d) A large tubule containing filaments (probably actin) and a line drawing showing the directionality of the filaments. Scale bars = 50 nm.

within the images were measured (Fig. 3c, d). In total, we found 37 large tubules, of which 30% appeared electron translucent and were either simple tubules or formed complexes with EVs and other membrane compartments (Fig. 3c). Approximately 70% of the tubules contained filaments and some of these appeared bent or hooked (Fig. 3d).

Category 9: pleomorphic membrane structures

The ejaculate consists of many more membranous compartments than the more easily categorized vesicles. These include pear-shaped membrane compartments and multiples thereof, large amorphous compartments that can be both empty looking and very electron dense (Fig. 4). These larger amorphous membrane compartments were often found in direct proximity to spermatozoa.

Category 10: vesicle sacs

The vesicle sacs consist of 6 or more single, double, triple (or more) vesicles arranged inside a larger membrane (Fig. 5a–c). The membranes of the largest vesicular sacs were broken and therefore not included in the size measurements. Notable is that vesicles with double membrane bilayers were also seen inside vesicle sacs.

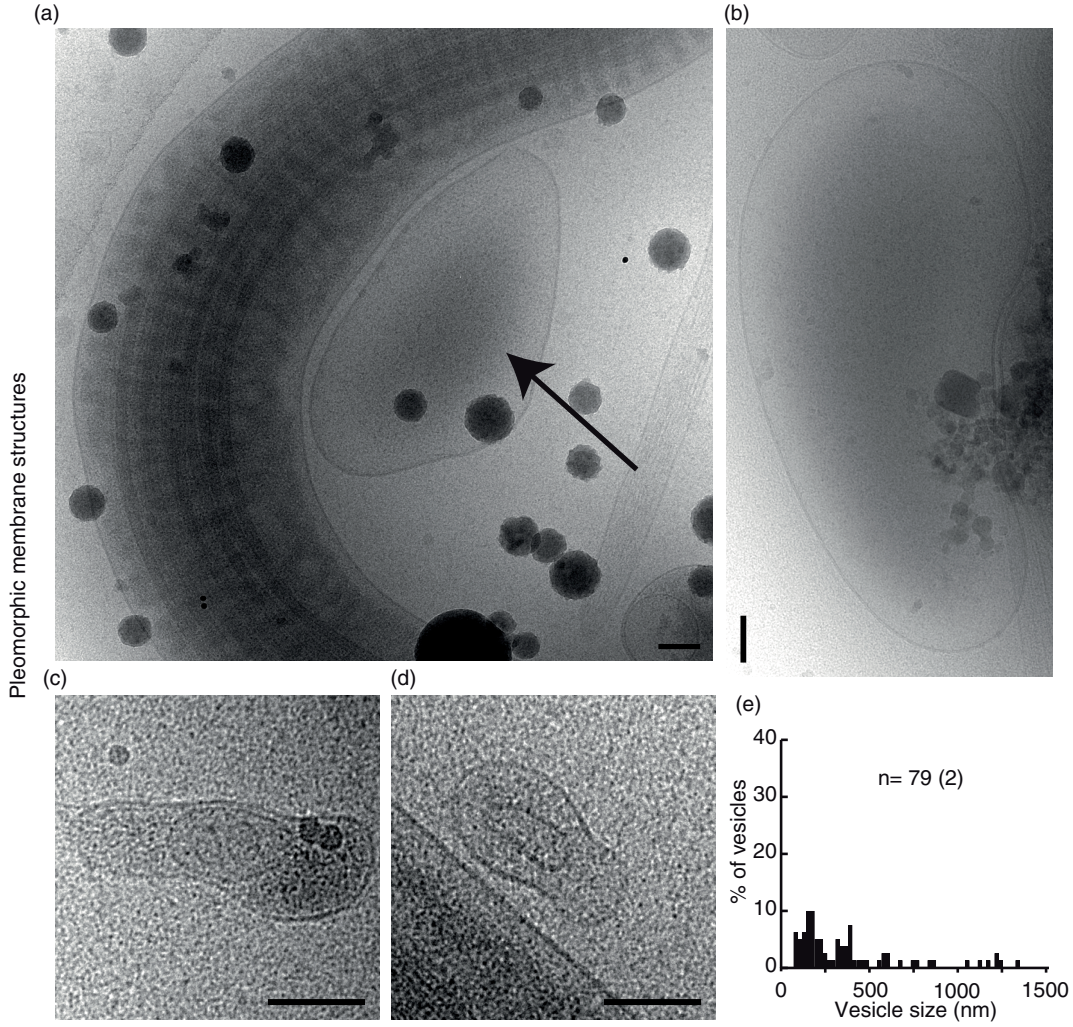

Fig. 4. Pleomorphic membrane structures – a diverse group of membrane compartments. (a) A large membrane-bound structure in close apposition to a sperm tail. (b) A large membrane compartment. (c) A tubular membrane structure containing a larger vesicle containing 2 smaller vesicles. (d) A figure 8-shaped membrane compartment containing a smaller oval membrane compartment. (e) Size distributions of pleomorphic membrane compartments. Scale bars = 50 nm.

Category 11: lamellar bodies

Large, complex, multilayered membrane structures were also visualized in the ejaculates (Fig. 5d, e).

Three additional features can be detected in the different EV and membrane compartment subcategories

Coated membranes

About 1.5% of the vesicles/membrane compartments show a coat extending from the lipid bilayer (n = 22 out of 1,432; Fig. 6a). This coat measure 9–17 nm, including the lipid bilayer, and was seen on a variety of vesicle subcategories (Fig. 6b–d).

Electron dense

About 8.7% of vesicles and membrane compartments showed a more electron dense interior, indicative of a lumen filled with cargo. These vesicles/compartments ranged in size from 61 nm (single vesicle) to 2,427 nm (pleomorphic membrane compartment). We have seen electron density inside double vesicles, double special vesicles, triple or more vesicles, incomplete vesicles as well as a small tubule.

Double membrane bilayers

In contrast to the double vesicles, these vesicles/compartments have 2 bilayers closely apposed to each other around the whole circumference (Fig. 6g). The double bilayer width varied between 7 and 15 nm (Fig. 6h). This feature is present on both small and large EVs, as well as tubules and pleomorphic membrane structures.

Vesicular fusion or budding with spermatozoa

In some images, we detected protrusions of the spermatozoon membrane, indicative of either vesicle fusion or budding. We measured the diameters of these protrusions

Citation: Journal of Extracellular Vesicles 2015, **4**: 28680 - http://dx.doi.org/10.3402/jev.v4.28680

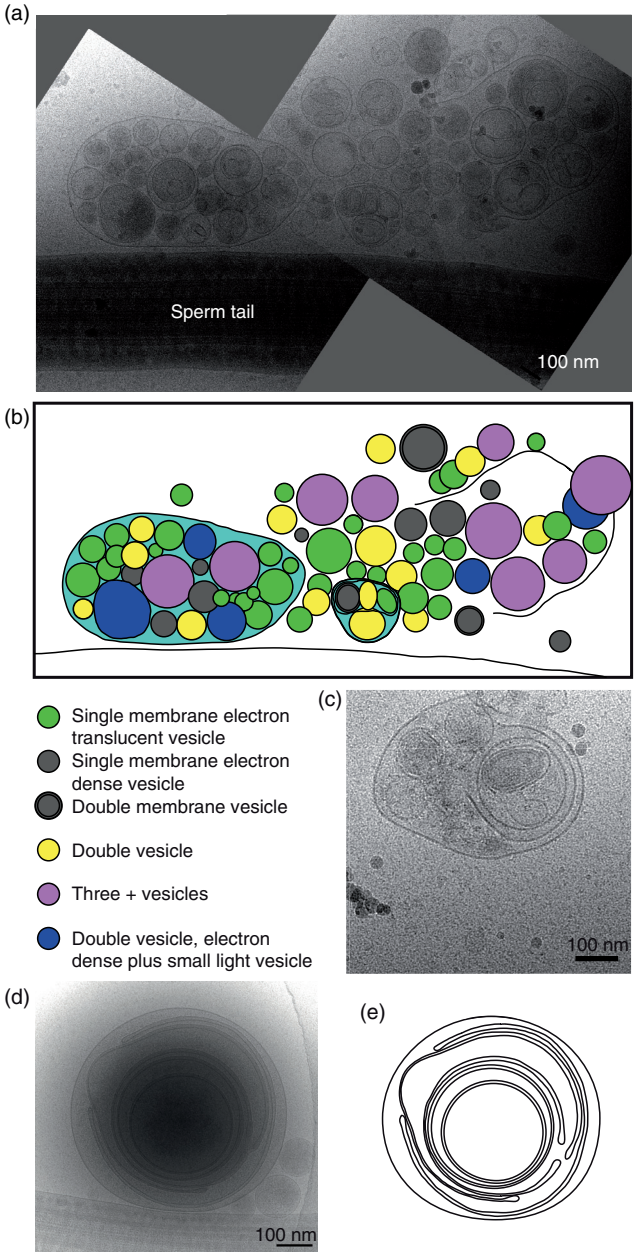

Fig. 5. Vesicle sacs and lamellar bodies. (a) Two overlapping cryo-electron micrographs showing a large collection of vesicles inside a membrane (left) and a similar ruptured structure (right). (b) A line drawing of the vesicles and membranes surrounding them in (a). Note that vesicles of different categories are present in the same vesicle sac (turquoise). (c) An example of a smaller, intact, vesicle sac. (d) A lamellar body showing multilayered membranes that are not always closed, shown as a line drawing in (e).

to examine if they correlated more with a specific vesicle subcategory. The protrusion diameters ranged from 60 to 350 nm (n = 7) and could thus be related to vesicles from any of the previously presented subcategories. Interestingly, we also could observe vesicles inside the sperm tail on 2 occasions (Fig. 7c).

Discussion

We have made an inventory of the extracellular structures in complete human ejaculates and discovered a highly diverse and complicated membranous environment outside the spermatozoa. Vesicles were defined as round, or close to round, structures carrying a lipid bilayer. Thus, the small electron dense particles were not considered to be true EVs, due to their lack of visible lipid bilayer. Cryo-electron tomography showed these particles to be located on top of the sample (Supplementary Fig. S1), where contaminating ice-crystals would be found. Other membrane structures, such as tubules and figure 8-shaped structures, were classified as compartments. In total, 11 different membranous relatively distinct morphological subcategories are described, and an additional 3 features can influence the morphology of any of these subcategories. Thus, a total of 88 different vesicles/compartment morphologies are possible. These results describe a membranous extracellular milieu that is extensively more complex than previously described. In a previous high-quality cryo-electron microscopy study of EVs isolated from human ejaculate, only 3 categories of EVs were found (33). Their EV isolates were composed of double special vesicles (50%), coated single vesicles (30–35%) and pleomorphic membrane structures (20–25%). In the present study, using unprocessed ejaculates, these 2 subcategories and "feature" entailed approximately 10% of the total membranous structures. It is unclear how universal these results are for other body fluids, but they should be considered when isolated vesicles are used for experimental purposes.

Diversity of EV structures

We show here an unprecedented diversity of extracellular structures in a single body fluid. However, in previous cryo-electron microscopy studies using different types of fluids, some of these structures have been described. For example, pleomorphic membrane compartments and tubular structures have been described in blood plasma (38,39), where multilayered vesicles can also be detected (39,40). Multilayered prostasomes have also been shown in thin-section electron microscopy (10,20). Tubular structures are also seen in human breast milk (41). Double and triple EVs from prion-infected cells were shown using electron tomography (42).

In theory, the structure of oval vesicles and tubular compartments could be induced by the compression experienced during blotting or freezing of the sample. However, the presence of vesicles elongating in different directions in the same image indicates that this is not the case. Furthermore, smaller oval EVs can be contained within perfectly round outer EVs, which should not be possible if the compression procedure had influenced the EV shapes (Fig. 2c, middle panel). We therefore suggest that biological molecules, such as lipid rafts (43), cytoskeletal

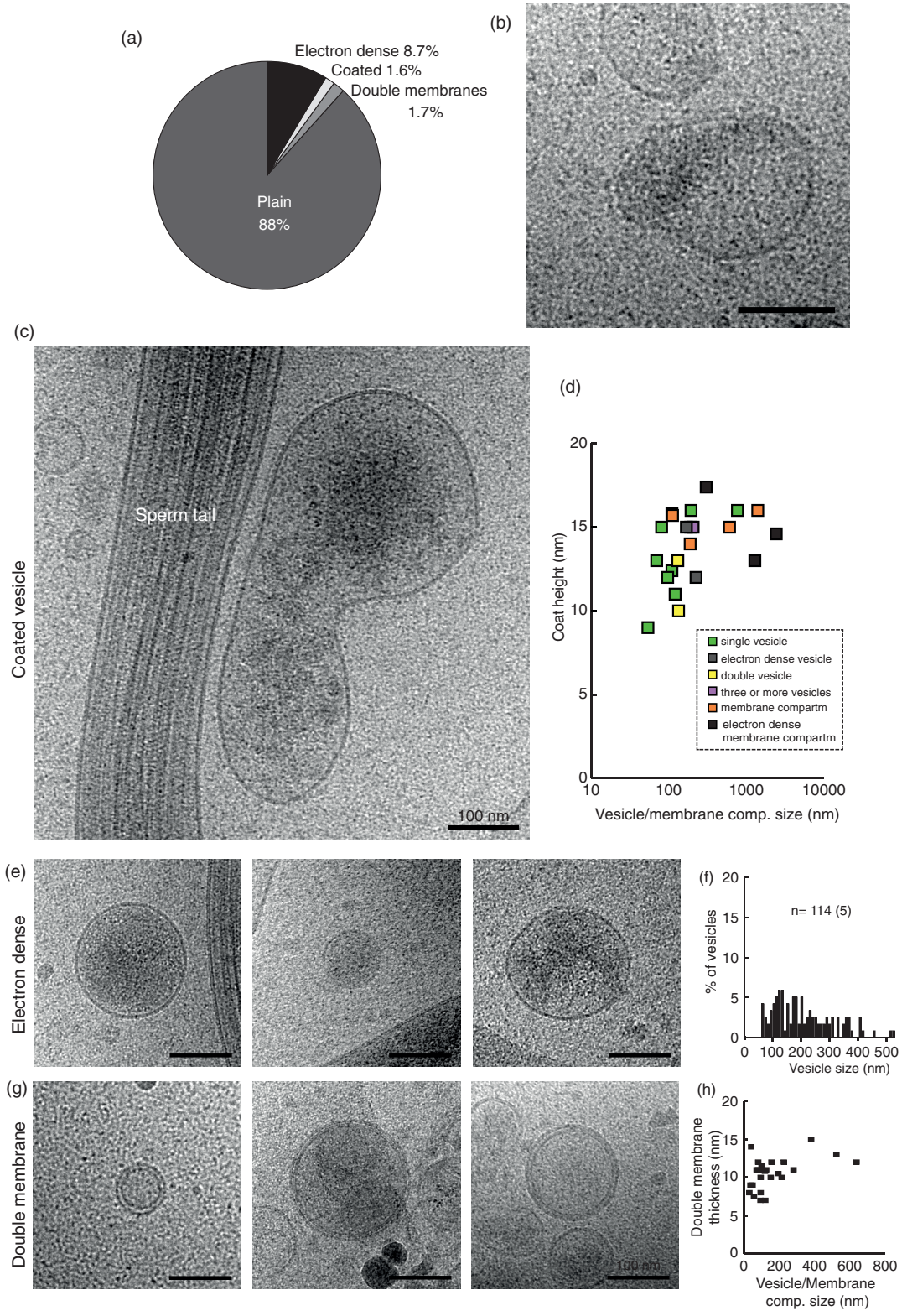

Fig. 6. Three special features can occur in any of the 11 subcategories. (a) Prevalence of the different features in the whole EV and membrane compartment population. (b and c) Membrane compartments with a coated membrane. (d) A logarithmic graph displaying the vesicle coat height as a correlation to the EV/compartment size. Colour coding shows that EVs of many categories, as well as membrane compartments, can be coated. (e) Three examples of electron dense vesicles. (f) The size distribution of electron dense vesicles. (g) Three examples of vesicles with double membrane bilayers. (h) The size distribution of all double bilayered EVs/compartments.

Citation: Journal of Extracellular Vesicles 2015, **4**: 28680 - http://dx.doi.org/10.3402/jev.v4.28680

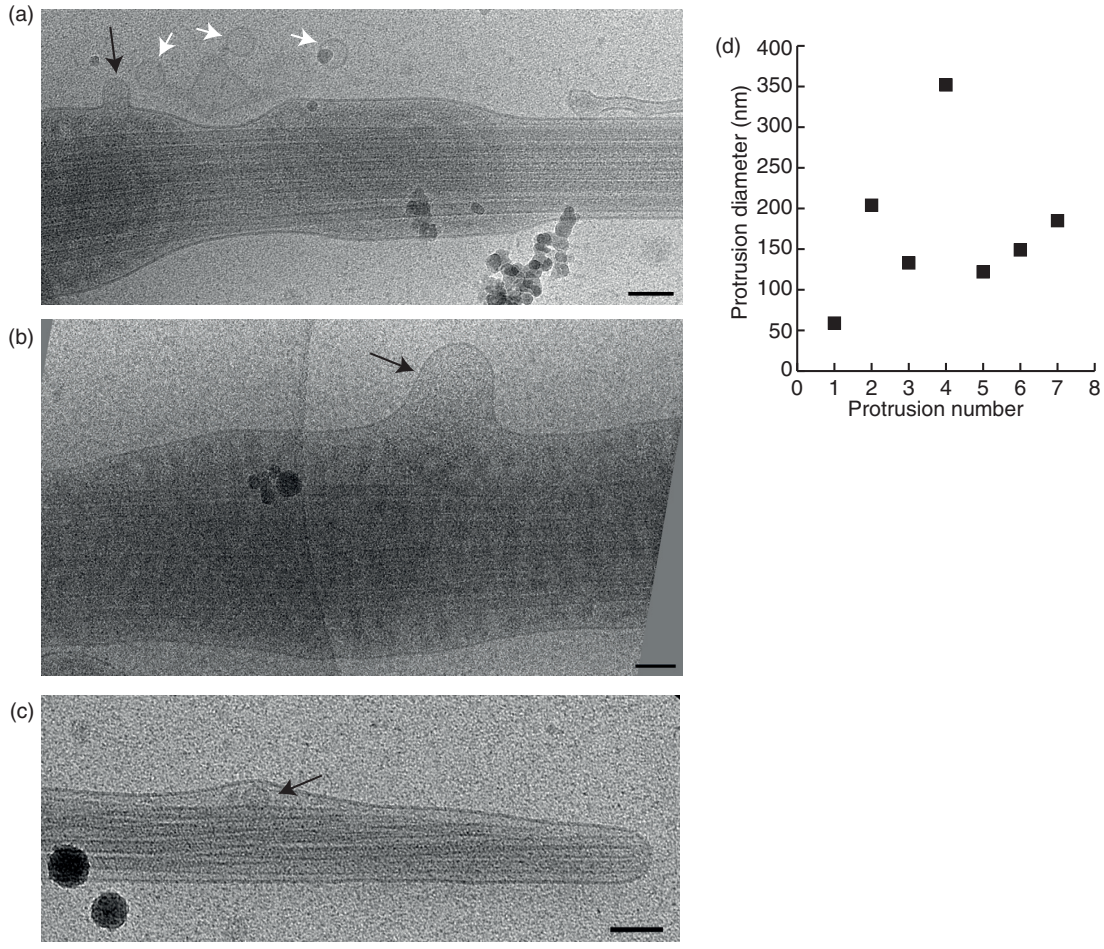

Fig. 7. Fusion or budding of vesicles to/from the sperm tail. (a) A small vesicle (black arrow) fusing into, or budding from the sperm tail. Three more vesicles of a similar size appear to be incoming/outgoing from this budding/fusion site. (b) A larger membrane protrusion (black arrow) looks like a budding/fusion event at the sperm tail. (c) Membrane deformation around this small vesicle (black arrow) shows that it is located inside the sperm end piece. (d) Measurements of all the membrane protrusions seen. Scale bars = 100 nm.

components and/or membrane shaping proteins, such as BAR-domain proteins (44), might influence the shape of the oval vesicles and tubules. It is also important to note that the studied samples have not been centrifuged or processed in any way prior to freezing, and therefore such procedures cannot explain the observed shapes.

The vesicle sac has previously been shown in cryo-electron microscopy of EVs derived from blood and *Dictyostelium discoideum* cell culture (37,38,45). They are of particular interest as it harbours EVs of different morphologies within the same membrane. This suggests that vesicles from several morphological subcategories can have the same subcellular origin. Vesicles of a similar size range as prostasomes have been described inside larger "storage vesicles" in prostate acinar cells that release cellular material to the extracellular space via apocrine secretion (12). It is likely that the vesicle sacs observed in the current study are indeed products of such secretion. Most noteworthy is that double membrane bilayer vesicles, a novel feature described in this study, can also be found within vesicle sacs. The double bilayer may be indicative of either (a) nuclear origin, (b) mitochondrial origin or (c) biogenesis through multiple steps of membrane fusion/fission. An alternative way of forming a double bilayer could be when two vesicles of similar size fuse to form a double vesicle, which could certainly be true for a fraction of the double bilayered EV population here described. However, EV fusion is unlikely to account for the whole population of double bilayered structures, as even tubules and pleomorphic membrane compartments can have double bilayers. The probability of them encountering a similarly shaped membrane compartment, and engulfing it, should be low.

Indeed, there are reasons to believe that there are even more EV subcategories in ejaculate than described here, as prostasomes from vasectomized men (ejaculate contains no EVs from testis or epididymis) contained two subpopulations of EVs with individual marker proteins (46).

Furthermore, two populations of prostasomes (of the single EV morphology) with different lipid compositions have also been described (47). The morphological subclasses presented here might thus consist of biochemically distinct subcategories, which fit well with the fact that some single EVs carry a surface coat and some do not.

Are EVs fusing or budding from the sperm tails?

The fusion of EVs to the spermatozoa has been shown to mostly happen at the sperm head and mid-region (48). Yet, we show here the presence of vesicles either budding or fusing from/with the sperm tail. Because of the nature of cryo-electron microscopy, imaging events frozen in time, it is impossible to determine whether the protrusions observed are events of vesicles budding or fusing, or both. Because of the varied sizes of protrusions from the sperm tails, a particular subcategory of vesicles could not be identified as more likely to fuse/bud from here. Our finding is also unexpected as Arienti and colleagues (49) showed that most prostasome fusion with spermatozoa occurs within 10 minutes of mixing the two components. We have processed and analysed no sample that was less than 60 minutes old before freezing. These two comparisons indicate that fusion might appear differently in complete ejaculate as compared to isolated vesicles added to washed spermatozoa.

In conclusion, we have here revealed that the human ejaculate carries a vastly diverse extracellular milieu of EVs and membrane compartments, some of which have never been described before. Future research will show if there is further EV diversity between individuals. Our study also unveils a need to complement research on isolated EVs with research on EVs without prior isolation to truly understand their role in human health and organismal biology, as a whole.

Acknowledgements

We thank The Boulder Lab for 3-D Electron Microscopy of Cells for the use of their electron microscopes (funded by Grant P41-RR000592) and the Electron Microscopy Unit at Sahlgrenska Academy, Gothenburg University, for helpful discussions. JLH was supported by a Sir Henry Wellcome Trust Postdoctoral Grant for part of this project. JL is partly funded by the VBG GROUP's Herman Krefting Foundation for Allergy and Asthma Research. This research was also funded by Swedish Research Council (K2014-85x-22504-01-3) and The Cancer Foundation (CAN 2012/690, 120772).

Conflict of interest and funding

JL owns stock in a company that is developing EVs as diagnostics and therapeutics.

References

1. Raposo G, Stoorvogel W. Extracellular vesicles: exosomes, microvesicles and friends. J Cell Biol. 2013;200:373–80.
2. Lässer C, Alikhani VS, Ekström K, Eldh M, Paredes PT, Bossios A, et al. Human saliva, plasma and breast milk exosomes contain RNA: uptake by macrophages. J Transl Med. 2011;9:9.
3. Lässer C, O'Neil SE, Ekerljung L, Ekström K, Sjöstrand M, Lötvall J. RNA-containing exosomes in human nasal secretions. Am J Rhinol Allergy. 2011;25:89–93.
4. Valadi H, Ekström K, Bossios A, Sjöstrand M, Lee JJ, Lötvall JO. Exosome-mediated transfer of mRNAs and microRNAs is a novel mechanism of genetic exchange between cells. Nat Cell Biol. 2007;9:654–9.
5. Crescitelli R, Lässer C, Szabó TG, Kittel A, Eldh M, Dianzani I, et al. Distinct RNA profiles in subpopulations of extracellular vesicles: apoptotic bodies, microvesicles and exosomes. J Extracell Vesicles. 2013;2:20677, doi: http://dx.doi.org/10.3402/jev.v2i0.20677
6. Skog J, Würdinger T, van Rijn S, Meijer DH, Gainche L, Curry WT, et al. Glioblastoma microvesicles transport RNA and proteins that promote tumour growth and provide diagnostic biomarkers. Nat Cell Biol. 2008;10:1470–6.
7. Xiao H, Lasser CL, Shelke GV, Wang J, dinger MR, Lunavat TR, et al. Mast cell exosomes promote lung adenocarcinoma cell proliferation – role of KIT-stem cell factor signaling. Cell Commun Signal. 2014;12:1–10.
8. Melo SA, Sugimoto H, O'Connell JT, Kato N, Villanueva A, Vidal A, et al. Cancer exosomes perform cell-independent microRNA biogenesis and promote tumorigenesis. Cancer Cell. 2014;26:707–21.
9. Ronquist G, Hedström M. Restoration of detergent-inactivated adenosine triphosphatase activity of human prostatic fluid with concanavalin A. Biochim Biophys Acta. 1977;483:483–6.
10. Ronquist G, Brody I, Gottfries A, Stegmayr B. An Mg2+ and Ca2+-stimulated adenosine triphosphatase in human prostatic fluid: part I. Andrologia. 1978;10:261–72.
11. Ronquist G, Brody I. The prostasome: its secretion and function in man. Biochim Biophys Acta. 1985;822:203–18.
12. Brody I, Ronquist G, Gottfries A. Ultrastructural localization of the prostasome – an organelle in human seminal plasma. Ups J Med Sci. 1983;88:63–80.
13. Belleannee C, Calvo E, Caballero J, Sullivan R. Epididymosomes convey different repertoires of microRNAs throughout the bovine epididymis. Biol Reprod. 2013;89:30.
14. Sullivan R, Frenette G, Girouard J. Epididymosomes are involved in the acquisition of new sperm proteins during epididymal transit. Asian J Androl. 2007;9:483–91.
15. Aalberts M, Stout TAE, Stoorvogel W. Prostasomes: extracellular vesicles from the prostate. Reproduction. 2013;147:R1–R14.
16. Palmerini CA, Saccardi C, Carlini E, Fabiani R, Arienti G. Fusion of prostasomes to human spermatozoa stimulates the acrosome reaction. Fertil Steril. 2003;80:1181–4.
17. Carlini E, Palmerini CA, Cosmi EV, Arienti G. Fusion of sperm with prostasomes: effects on membrane fluidity. Arch Biochem Biophys. 1997;343:6–12.
18. Burden HP. Prostasomes – their effects on human male reproduction and fertility. Hum Reprod Update. 2006;12:283–92.
19. Arienti G, Carlini E, Saccardi C, Palmerini CA. Role of human prostasomes in the activation of spermatozoa. J Cell Mol Med. 2004;8:77–84.
20. Ronquist G. Prostasomes are mediators of intercellular communication: from basic research to clinical implications. J Intern Med. 2011;271:400–13.
21. Stegmayr B, Ronquist G. Promotive effect on human sperm progressive motility by prostasomes. Urol Res. 1982;10:253–7.
22. Park K-H, Kim B-J, Kang J, Nam T-S, Lim JM, Kim HT, et al. Ca2+ signaling tools acquired from prostasomes are required

for progesterone-induced sperm motility. Sci Signal. 2011; 4:ra31.
23. Andersson E, Sørensen OE, Frohm B, Borregaard N, Egesten A, Malm J. Isolation of human cationic antimicrobial protein-18 from seminal plasma and its association with prostasomes. Hum Reprod. 2002;17:2529–34.
24. Carlsson L, Påhlson C, Bergquist M, Ronquist G, Stridsberg M. Antibacterial activity of human prostasomes. Prostate. 2000;44:279–86.
25. Fernández JA, Heeb MJ, Radtke KP, Griffin JH. Potent blood coagulant activity of human semen due to prostasome-bound tissue factor. Biol Reprod. 1997;56:757–63.
26. Kelly RW, Holland P, Skibinski G, Harrison C, McMillan L, Hargreave T, et al. Extracellular organelles (prostasomes) are immunosuppressive components of human semen. Clin Exp Immunol. 1991;86:550–6.
27. Tarazona R, Delgado E, Guarnizo MC, Roncero RG, Morgado S, Sánchez-Correa B, et al. Human prostasomes express CD48 and interfere with NK cell function. Immunobiology. 2011;216:41–6.
28. Tavoosidana G, Ronquist G, Spyros D, Yan J, Carlsson L, Wu D, et al. Multiple recognition assay reveals prostasomes as promising plasma biomarkers for prostate cancer. Proc Natl Acad Sci U S A. 2011;108:8809–14.
29. Bordi F, Cametti C, De Luca F, Carlini E, Palmerini CA, Arienti G. Hydrodynamic radii and lipid transfer in prostasome self-fusion. Arch Biochem Biophys. 2001;396:10–5.
30. Arvidson G, Ronquist G, Wikander G. Human prostasome membranes exhibit very high cholesterol/phospholipid ratios yielding high molecular ordering. Biochim Biophys Acta. 1989;984:167–73.
31. Mielanczyk L, Matysiak N, Michalski M, Buldak R, Wojnicz R. Closer to the native state. Critical evaluation of cryo-techniques for transmission electron microscopy: preparation of biological samples. Folia Histochem Cytobiol. 2014;52:1–17.
32. Hoenger A. High-resolution cryo-electron microscopy on macromolecular complexes and cell organelles. Protoplasma. 2014;251:417–27.
33. Poliakov A, Spilman M, Dokland T, Amling CL, Mobley JA. Structural heterogeneity and protein composition of exosome-like vesicles (prostasomes) in human semen. Prostate. 2009;69: 159–67.
34. World Health Organization. WHO laboratory manual for the examination and processing of human semen. 5th ed. 2010. p. 1–286. [cited 1 Sept 2015]. Available from: http://whqlibdoc.who.int/publications/2010/9789241547789_eng.pdf?ua=1
35. Höög JL, Bouchet-Marquis C, McIntosh JR, Hoenger A, Gull K. Cryo-electron tomography and 3-D analysis of the intact flagellum in *Trypanosoma brucei*. J Struct Biol. 2012;178: 189–98.
36. Höög JL, Lacomble S, O'Toole ET, Hoenger A, McIntosh JR, Gull K. Modes of flagellar assembly in *Chlamydomonas reinhardtii* and *Trypanosoma brucei*. eLife. 2014;3:e01479.
37. Mastronarde DN. Automated electron microscope tomography using robust prediction of specimen movements. J Struct Biol. 2005;152:36–51.
38. Arraud N, Linares R, Tan S, Gounou C, Pasquet JM, Mornet S, et al. Extracellular vesicles from blood plasma: determination of their morphology, size, phenotype and concentration. J Thromb Haemost. 2014;12:614–27.
39. Yuana Y, Koning RI, Kuil ME, Rensen PCN, Koster AJ, Bertina RM, et al. Cryo-electron microscopy of extracellular vesicles in fresh plasma. J Extracell Vesicles. 2013;2:21494, doi: http://dx.doi.org/10.3402/jev.v2i0.21494
40. Issman L, Brenner B, Talmon Y, Aharon A. Cryogenic transmission electron microscopy nanostructural study of shed microparticles. PLoS One. 2013;8:e83680.
41. Zonneveld MI, Brisson AR, van Herwijnen MJC, Tan S, van de Lest CHA, Redegeld FA, et al. Recovery of extracellular vesicles from human breast milk is influenced by sample collection and vesicle isolation procedures. J Extracell Vesicles. 2014;3:24215, doi: http://dx.doi.org/10.3402/jev.v3.24215
42. Coleman BM, Hanssen E, Lawson VA, Hill AF. Prion-infected cells regulate the release of exosomes with distinct ultrastructural features. FASEB J. 2012;26:4160–73.
43. Diaz-Rohrer B, Levental KR, Levental I. Rafting through traffic: membrane domains in cellular logistics. Biochim Biophys Acta. 2014;1838:3003–13.
44. Mim C, Unger VM. Membrane curvature and its generation by BAR proteins. Trends Biochem Sci. 2012;37:526–33.
45. Tatischeff I, Larquet E, Falcón-Pérez JM, Turpin P-Y, Kruglik SG. Fast characterisation of cell-derived extracellular vesicles by nanoparticles tracking analysis, cryo-electron microscopy, and Raman tweezers microspectroscopy. J Extracell Vesicles. 2012;1:19179, doi: http://dx.doi.org/10.3402/jev.v1i0.19179
46. Aalberts M, van Dissel-Emiliani FMF, van Adrichem NPH, van Wijnen M, Wauben MHM, Stout TAE, et al. Identification of distinct populations of prostasomes that differentially express prostate stem cell antigen, annexin A1, and GLIPR2 in humans. Biol Reprod. 2012;86:82.
47. Brouwers JF, Aalberts M, Jansen JWA, van Niel G, Wauben MH, Stout TAE, et al. Distinct lipid compositions of two types of human prostasomes. Proteomics. 2013;13:1660–6.
48. Aalberts M, Sostaric E, Wubbolts R, Wauben MW, Nolte-'t Hoen EN, Gadella BM, et al. Spermatozoa recruit prostasomes in response to capacitation induction. Biochim Biophys Acta. 2013;1834:2326–35.
49. Arienti G, Carlini E, Palmerini CA. Fusion of human sperm to prostasomes at acidic pH. J Membr Biol. 1997;155:89–94.